RF AMPLITUDE AND PHASE STABILIZATION FOR A SUPERCONDUCTING LINEAR ACCELERATOR BY FEEDBACK STABILIZATION TECHNIQUES*

L.R. Suelzle
High Energy Physics Laboratory, Stanford University
Stanford, California

INTRODUCTION

Of the properties[1,2] of a superconducting electron linac, one of the most important for energy and current stability of the exit beam is the continuous or long-duty-cycle property. Conventional linacs are restricted to short-duty-cycle operation in which case such exit-beam properties as spread in energy are dominated by the transient conditions associated with the short duty cycle. Under these conditions, utilization of feedback stabilization techniques to stabilize the rf accelerating fields in the accelerating structure can be very difficult. In this paper, I would like to discuss some of the feedback stabilization techniques being examined and tested at Stanford and to describe how the high-Q characteristic of a superconducting linac can simplify some of the feedback control problems.

DRIVING THE ACCELERATOR STRUCTURE

In the superconducting electron linac (SEL), the operating conditions will be typically that of extreme beam loading, where the power supplied to the beam is much larger than the power lost to the cavity structure. In the conventional linac, a beam loading of 50% is considered "heavy loading." The problems of matching the rf sources to the driving-point impedances are therefore very different for the SEL. Other operations such as "drifting" a beam through an unpowered section or such as reverse-phase operation have a very different significance for the SEL.

The beam loading of the accelerating structure can be examined by considering the resonant circuit shown in Fig. 1. It is assumed throughout this discussion that the structure is a standing wave structure. The cavity structure (considering only one mode) is represented by the parallel resonant circuit with admittance

$$Y_c = G_c \left[1 + j\, 2Q_o\, \delta\right] \quad , \tag{1}$$

where G_c is the equivalent shunt conductance, Q_o is the unloaded quality factor for the structure, and δ is the tuning decrement $(\omega - \omega_o)/\omega_o$. The power source and transmission line are represented by the voltage source $\vec{V}_g$ [amplitude $V_g = |\vec{V}_g|$ and phase $\mathrm{Arg}(\vec{V}_g)$] with impedance R_g (assumed to be real). The coupling is represented by a

---

*Work supported in part by the U.S. Office of Naval Research, Contract [NONR 225(67)].

1. P.B. Wilson, Linear Accelerators, P. Lapostolle and A. Septier, editors, Chapter 5.1 (to be published).

2. H.A. Schwettman, J.P. Turneaure, W.M. Fairbank, T.I. Smith, M.S. McAshan, P.B. Wilson, and E.E. Chambers, IEEE Trans. Nucl. Sci. NS-14, No. 3, 336 (1967).

transformer of turns-ratio n. $\vec{V}_i$ is the voltage of the incident wave and $\vec{V}_r$ is the voltage of the returning wave. P_i and P_r, the incident and returning power, are given by $P_i = V_i^2/2R_g$ and $P_r = V_r^2/2R_g$. The beam effects are represented by the current generator $\vec{I}_b$. For a relativistic and well-bunched beam, the amplitude I_b is approximately equal to $2I_o$ where I_o is the dc component of the beam current. The cavity voltage $\vec{V}_c$ is computed by summing the voltages produced when each of the generators is considered independently. The result is given by

$$\vec{V}_c = n(1 + \Gamma)\vec{V}_i - \frac{n^2 R_g \vec{I}_b}{1 + n^2 R_g Y_c} \tag{2}$$

where

$$\Gamma = \frac{1 - n^2 R_g Y_c}{1 + n^2 R_g Y_c} \quad . \tag{3}$$

The coupling coefficient β is given by

$$\beta = (n^2 R_g G_c)^{-1} \quad . \tag{4}$$

At resonance ($\delta = 0$), Γ is equal to $(\beta - 1)/(\beta + 1)$. The acceleration voltage V_a is given by

$$V_a = \frac{-\vec{V}_c \cdot \vec{I}_b}{I_b} = -V_c \cos\varphi \quad , \tag{5}$$

where φ is the phase angle between the cavity voltage $\vec{V}_c$ and the current $\vec{I}_b$. For a properly phased beam, $\varphi = 180^o$. From this point on, let us consider only the on-resonance, beam-in-phase case. Let us also assume that $n^2 R_g G_c \ll 1$. This is the extremely overcoupled case of $\beta \gg 1$. In this case,

$$V_a = 2nV_i - n^2 R_g I_b \quad , \tag{6}$$

and

$$V_r = V_i - nR_g I_b \quad . \tag{7}$$

Let us further assume that the transformer turns-ratio n is chosen so that $V_r = 0$ at $I_b = I_b(\max)$ and $V_i = V_i(\max)$. Remembering that $I_b = 2I_o$ and $V_a = nV_i$,

$$n^2 = \frac{V_a(\max)}{2R_g I_o(\max)} \quad . \tag{8}$$

For this transformer turns-ratio, V_a and P_r become

$$V_a = 2V_a(\max)\left[\frac{P_i}{P_i(\max)}\right]^{\frac{1}{2}} - V_a(\max)\frac{I_o}{I_o(\max)} \quad , \tag{9}$$

and

$$P_r = P_i + \left(\frac{I_o}{I_o(\max)}\right)^2 P_i(\max) - 2P_i(\max)\frac{I_o}{I_o(\max)}\left[\frac{P_i}{P_i(\max)}\right]^{\frac{1}{2}} . \tag{10}$$

V_a and P_r are plotted in Figs. 2a and 2b for the two special cases of $I_o = 0$ and $I_o = I_o(\max)$.

From the curves in Figs. 2a and 2b, we see that with $I_o = 0$ the power P_i required to produce the cavity voltage $V_a(\max)$ is $P_i = P_i(\max)/4$. Also, for $I_o = 0$, P_i approximately equals P_r. When $I_o = I_o(\max)$, to obtain V_a equal to 0, P_r equals P_i which equals $P_i(\max)/4$. If $P_i = 0$ (source turned off) and $I_o = I_o(\max)$, V_a equals $-V_a(\max)$ and P_r equals $P_i(\max)$. Therefore, the concept of "drifting" a beam through an unpowered section of accelerator takes on a different significance. It is very important that the source end of the transmission line is always reverse-terminated in a load capable of dissipating a power as large as $P_i(\max)$ (e.g. an isolator or a circulator plus a load). If a section of the accelerator cannot be powered, it will be necessary to detune the structure so that the energy $V_a(\max)$ is not lost. The amount of energy lost can also be reduced by increasing the amount of overcoupling.

We also notice from Figs. 2a and 2b that the operation in which the generator is reverse-phased should be avoided since the cavity voltages and return power will become excessive. Reverse phasing is sometimes used with conventional linacs to obtain high currents with low final beam energies.

RF STABILITY REQUIREMENTS

With the continuous wave or long-duty-cycle capability of the SEL, the transient effects no longer limit the amplitude and phase stability of the accelerating fields. The Stanford group has set a design goal for resolution in energy of the exit beam of $\Delta E_f/E_f \leq 10^{-4}$. The design goal for stability of the energy gain in a single accelerating structure has been set at $\Delta E/E \leq 10^{-4}$.

The energy gain through a section of the accelerator is described by

$$E = E_o \cos \varphi \quad , \tag{11}$$

where E_o is the energy gain when the phasing angle φ is zero. Let us assume that the beam has a phase spread (phase bucket) of $\Delta\varphi$ centered at a phasing angle φ_o ; then the spread in the energy gain can be approximated by

$$\left[\frac{\Delta E}{E}\right]^2 \approx \left[\frac{\Delta E_o}{E_o}\right]^2 + \left[\frac{(\Delta\varphi + 2|\varphi_o|)^2}{8}\right]^2 \quad . \tag{12}$$

With an amplitude stability $\Delta E_o/E_o \approx \pm 7 \times 10^{-5}$, a phase spread $\Delta\varphi \approx 1^o$ (determined by the injector conditions), and a phasing angle $\varphi_o \approx \pm 0.2^o$, $\Delta E/E$ is approximately 10^{-4}. We are therefore attempting to hold the amplitude of the rf to a stability of $\pm 7 \times 10^{-5}$ and the phase to a stability of $\pm 0.2^o$.

FEEDBACK CONTROL SYSTEM

In order to obtain the desired amplitude and phase stability in the accelerator structure in the presence of large perturbations such as beam loading or frequency shifts, it is necessary to use feedback control. In Fig. 3 a simplified block diagram of the feedback control system that has been constructed and studied at Stanford is shown. The rf field in one of the excited cavities of the accelerating structure is sampled by a pickup probe which couples a relatively small amount of power (0.1 to 1.0 W) to the amplitude and phase detection circuitry. A detector diode, which will be discussed in a subsequent section of this paper, provides a voltage which is proportional to the rf amplitude. This voltage is compared with a reference voltage

which may be a dc or pulse signal. The amplified error signal is then used to control a PIN diode attenuator in the rf input line to a klystron power amplifier.

The phase of the rf is measured relative to a reference signal which is common to the entire accelerator. The phase setting is adjusted by means of a phase shifter located between the reference phase and the phase detector. The problem of selecting the phase angle so that the cavity voltage is in phase with the bunched electron beam will not be discussed in this paper. Once a suitable phase is selected, it is the function of the feedback control system to maintain the phase alignment. The error signal from the phase detector is used to control an electronic phase shifter in the rf input line to the klystron amplifier.

With the large mismatch condition that can exist with the power feed system, it is necessary to provide an isolator (or circulator and load) to absorb the power returning from the structure. As discussed earlier, the isolator must be capable of dissipating the maximum available power from the generator.

The reflectometer shown in Fig. 3 compares the phase of the return signal with the incident signal in the power feed to the accelerator structure. This phase comparison provides a measure of how well the structure is tuned to the driving frequency. The signal from the reflectometer can be used in the automatic tuning of the structure.

Shown in Fig. 4 is the phase shifter circuitry used in our prototype test. A variable reactance at one port of a four-port circulator varies the phase of the reflected rf signal at that port. The variable reactance is produced by varying the reverse bias on a diode. The phase shifting range is expanded by resonating the diode capacitance with an inductance.[3]

AMPLITUDE DETECTION

Shown in Fig. 5 is a diagram of the amplitude detection circuit. A coupling probe (magnetic coupling) provides a 0.1 to 1.0 W signal for the amplitude and phase detection circuitry. A Hot Carrier diode operating as a large-signal detector (peak reading with negligible power dissipation in the diode) provides a voltage proportional to the amplitude of the rf signal. The diode is housed in a structure which has a small amount of tuning capability to compensate for the effective capacitance of the diode and is temperature stabilized to better than $0.2^{\circ}C$. The temperature coefficient for the Hot Carrier diode depends on the particular loading conditions and has been measured at approximately 1 $mV/^{\circ}C$ for our conditions (output voltage of 10 V at the 1 W level). Since our amplitude stability requirements are predominantly short-term requirements of the order of minutes, long-term effects such as diode aging are not considered to be vital problems.

The problems of mismatches or changing impedance of the transmission line affecting the amplitude stability can be minimized by taking advantage of the low output impedance provided by the undercoupled magnetic coupling ($\simeq 0.5\ \Omega$). This is done by locating the diode at an integer number of transmission-line half wavelengths from the coupling. We have used a PIN diode as a controllable perturbation on the system and have adjusted the line length between the diode and the coupling probe to minimize the amplitude variations produced by the perturbation. Since a change in the amplitude level at the diode will change the reactive loading produced by the diode, the problem of holding the phase constant with changes in amplitude is minimized by locating the diode at this low-impedance point.

---

3. R.H. Hardin, E.J. Downey, and J. Munushian, Proc. IRE 48, 944 (1960).

PHASE DETECTOR

The phase detector circuitry is summarized in Fig. 6. Signals $\vec{B}$, with amplitude B, and $\vec{A}$, with amplitude A and phase angle φ relative to $\vec{B}$, are combined in a four-port, 3 dB hybrid (racetrack hybrid). The vectorial sums $\vec{A} + \vec{B}$ and $\vec{A} - \vec{B}$, which are obtained at the other two ports, are detected by linear detectors with detection efficiencies k_1 and k_2 respectively. The detected signals are subtracted to produce the video signal E_v where

$$E_v = k_1 \left[A^2 + B^2 - 2AB \cos \varphi\right]^{\frac{1}{2}} - k_2 \left[A^2 + B^2 + 2AB \cos \varphi\right]^{\frac{1}{2}} \quad . \tag{13}$$

With neither $\vec{A}$ nor the reference signal $\vec{B}$ modulated, E_v is a dc signal which, for $k_1 = k_2$, is null at φ equal to 90 or 270°. Should the detection efficiencies or detection power law characteristics for one diode change relative to the other diode, the null would be found at a different value of φ. For 0.1° stability, the two diodes must track to about one part in 300.

The problem of the extreme tracking requirement for the diodes can be removed by modulating the reference signal $\vec{B}$. For $B = B_o + B_1 \sin \omega_m t$, $\varphi = \pi/2 - \alpha$, and $A \gg B_o$, E_v becomes

$$E_v = (k_1 + k_2) B_1 \sin \alpha \sin \omega_m t + (k_1 - k_2) \frac{B_o}{A} B_1 \sin \omega_m t$$

$$+ \frac{(k_2 - k_1) B_1^2}{4A} \cos 2\omega_m t + \text{dc terms} \quad . \tag{14}$$

If we consider only those terms with frequency ω_m, we are left with the first two terms in Eq. (14). If

$$\left(\frac{k_1 - k_2}{k_1 + k_2} \right) \frac{B_o}{A} < 10^{-3} \quad ,$$

then the null in the amplitude of frequency ω_m will occur at $-0.1 < \alpha < 0.1°$. The ratio B_o/A is made small by suppressing the carrier ($B_o \ll B_1$) and by making A large compared with B_1. The suppressed carrier reference signal method is referred to as the homodyne phase detection system.[4]

For our tests, we have used a 100 kHz modulation frequency with a doubly-balanced modulator which suppressed the carrier at 952 MHz to -20 dB ($B_o/B_1 \approx 0.1$). The ratio B_1/A was less than 0.1 and the diode-tracking term $(k_1 - k_2)/(k_1 + k_2)$ was less than 0.05.

FEEDBACK DYNAMICS

The high-Q characteristic of the superconducting accelerating structure leads to a great simplification in the feedback control dynamics when the system is compared with the conventional room temperature structure. For a loaded Q of 10^8 at a frequency of 1 GHz, the structure has a time constant of 0.032 sec (video bandwidth of 5 Hz). The time constants of the other elements in the control loops (amplifiers, PIN diode

---

4. S.D. Robertson, Bell System Tech. J. 28, 99 (1949).

attenuator, varactor phase shifters, etc.) will be much smaller than 32 msec, typically in the microsecond range (100 kHz video bandwidth). Consequently, the gain-frequency curve for the control loop can be a -6 dB/octave roll-off with unity-gain crossover at 10 kHz which will be shown later to yield more than an adequate gain-bandwidth product for the control loop.

For the room-temperature linear accelerators, where the loaded Q may be of the order of 10^4 and where pulse lengths are relatively short, the response characteristics of the control loop become more complex because of a much higher gain-bandwidth requirement. A modulated phase reference signal, for example, may not be usable because of the bandwidth limitation of a modulated system. The transient problems are further complicated when the spectrum of video frequencies is sufficiently large that one or more of the adjacent resonant modes of the multicavity accelerating structure can be excited.[5]

For the control loops for the superconducting accelerator at Stanford, we have tentatively selected a gain-bandwidth product of 10^4 Hz for both the amplitude and phase control loops. Direct current loop gains of 10^5 for the amplitude loop and 10^3 for the phase loop will be more than sufficient to handle the perturbations inside the loops.

In Fig. 7 is shown the loop diagram for the amplitude control loop with the appropriate transfer functions. A_o is the dc loop gain (selected at 10^5) and T_1 is the dominant pole in the system (≈ 1.6 sec). A zero at $S = 1/T_2$ and $T_2 \approx T_c$, where T_c is the cavity time constant, maintains the roll-off at -6 dB/octave. E_b represents the electron beam component to the cavity voltage E_c. Shown in Fig. 8 are the approximate time responses for the transient conditions from initial turn-on to the maximum operating cavity voltage and beam current. With the initial turn-on of the reference voltage, the power incident to the accelerator structure is turned on to the maximum available power which is assumed, for discussion, to be slightly higher than $P_i(\max)$. The cavity voltage E_c changes exponentially toward the final value $2V_a(\max)$. When the voltage reaches the desired value of $V_a(\max)$ (in approximately 0.7 of a filling time), the control loop comes out of saturation and regulates the cavity voltage to $V_a(\max)$. A power of $P_i(\max)/4$ is required to maintain the voltage of $V_a(\max)$ with the coupling parameters discussed earlier in this paper.

When the beam current is turned on to $I_o(\max)$, the control loop increases the power to the $P_i(\max)$ level in approximately 16 μsec. During this beam turn-on transient, the cavity voltage falls by a part in 2000 and recovers to within a part in 10^4 in approximately 100 μsec. The transient dip in the cavity voltage when the beam is turned on limits the minimum cavity voltage at which the regulating system can continue to regulate with a step change in the beam current from 0 to $I_o(\max)$.

TEST RESULTS

The amplitude and phase control loops were tested with a room-temperature five-cavity, 952 MHz, copper accelerating structure (power input of 100 W and less). Redundant amplitude and phase detection units were used to check the stability of the system. The desired stabilities in amplitude and phase were achieved even though the mechanical stability of our test coupling probes would not be adequate for the final accelerator. High-stability coupling probes are currently being designed.

---

5. R.A. Jameson, Los Alamos Scientific Laboratory Report LA-3372 (1965).

A five-cavity, lead-plated-copper, 952 MHz accelerating structure was cooled to $4.2^{o}K$ and yielded an unloaded Q of 10^{8}. Shown in Fig. 9 are oscilloscope traces of the cavity voltage, the square root of the incident power, and the square root of the reflected power in response to a pulsed reference signal. The cavity was critically coupled to the generator ($Q_L = 5 \times 10^7$) and stabilized in amplitude and phase. Although this was only the initial test of the system with a superconducting structure (no beam), the performance met our expectations.

ACKNOWLEDGEMENTS

The author expresses his appreciation to J. Arnold, G. Ramian, and H. Schwarz for their roles in the designing, developing, and testing of the system presented in this paper. Valuable discussions with J. Weaver were greatly appreciated.

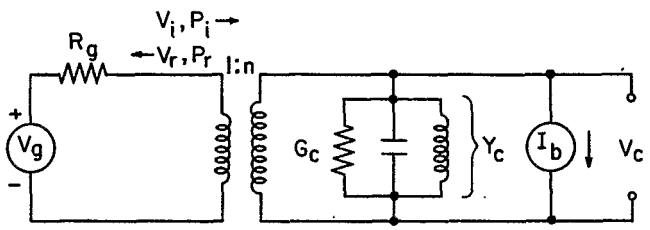

$$\beta = (n^2 G_c R_g)^{-1} \qquad I_b \approx 2 I_o$$

$$Y_c = G_c (1 + j 2 Q_o \delta) \qquad \delta = \frac{\omega - \omega_o}{\omega_o}$$

Fig. 1. Equivalent circuit for a standing wave cavity loaded by a relativistic beam.

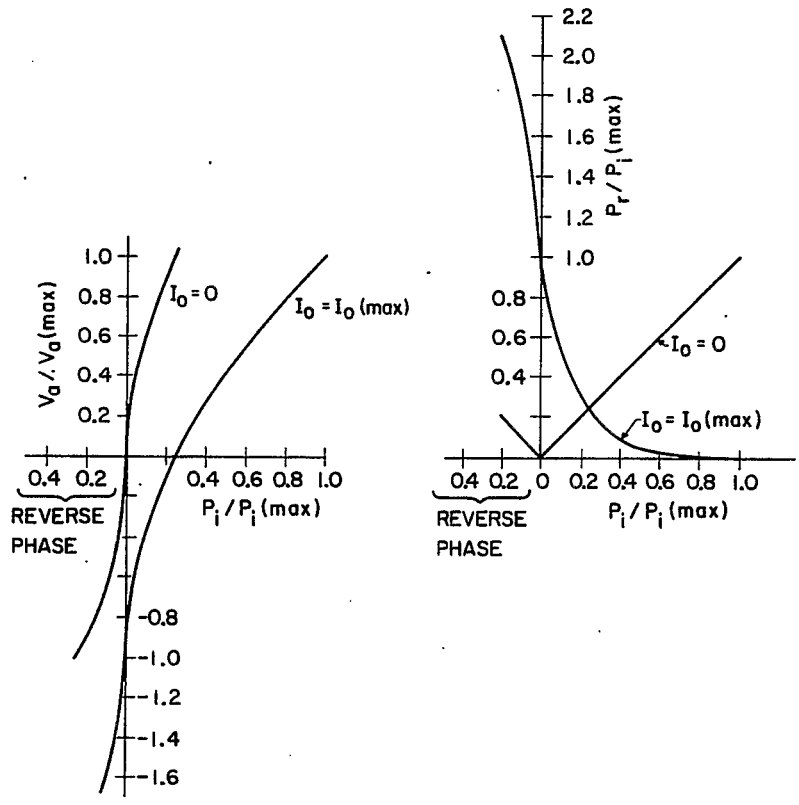

Fig. 2. Voltage gain V_a and the return power P_r as a function of the incident power P_i for values of beam current $I_o = 0$ and $I_o = I_o(max)$. The coupling to the cavity has been selected for optimization at $V_a = V_a(max)$ and $I_o = I_o(max)$.

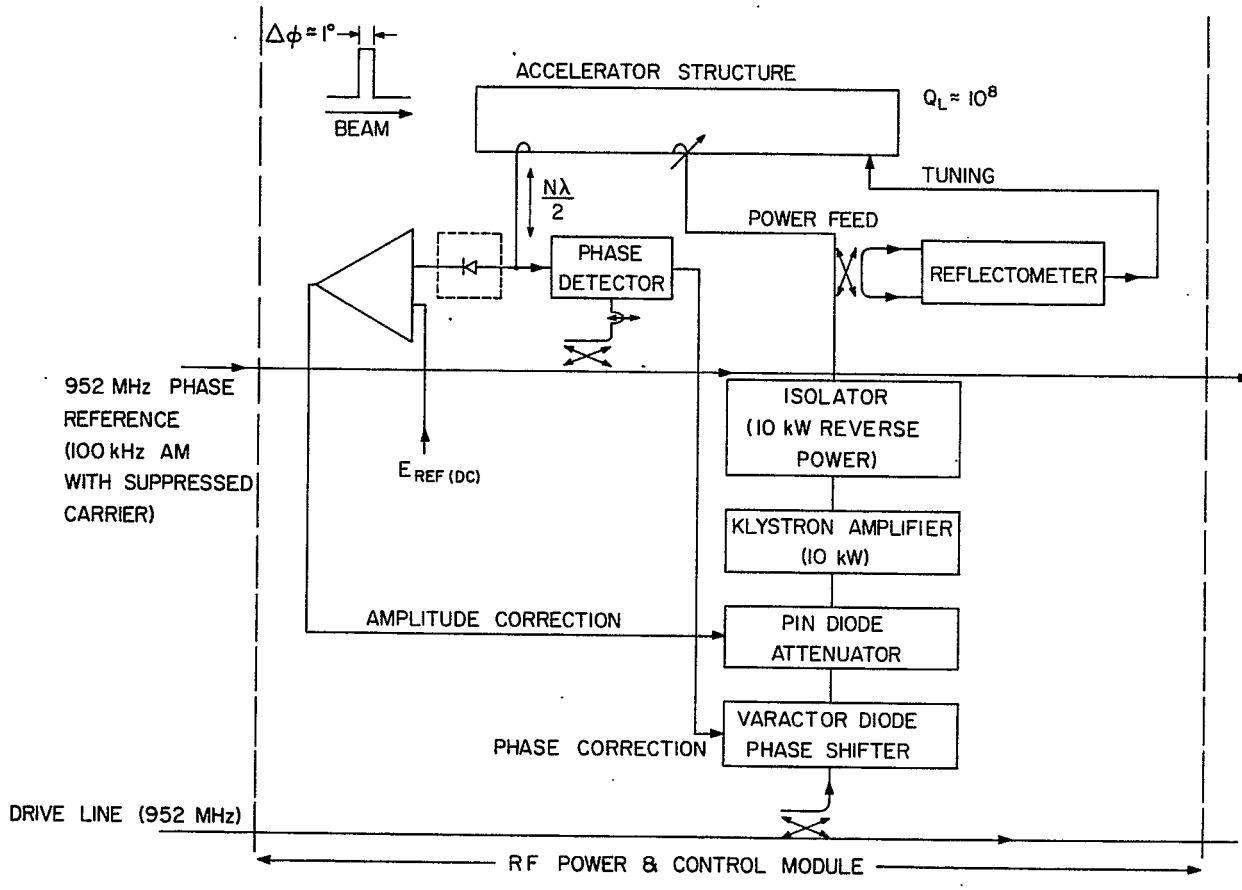

Fig. 3. Block diagram of amplitude and phase control loops.

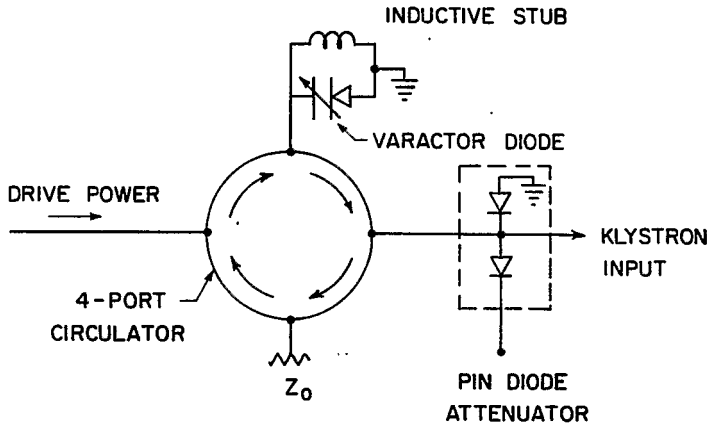

Fig. 4. Prototype varactor diode phase shifter and PIN diode attenuator.

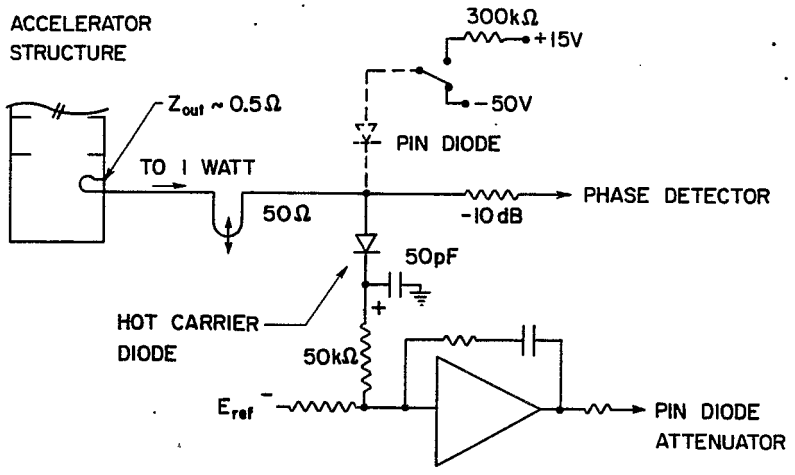

Fig. 5. Amplitude detection circuitry.

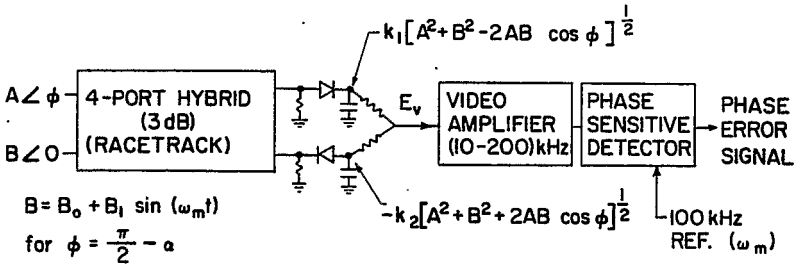

$B = B_o + B_1 \sin(\omega_m t)$

for $\phi = \frac{\pi}{2} - \alpha$

$$E_v = (k_1+k_2)B_1 \sin\alpha \sin(\omega_m t) + (k_1-k_2)\frac{B_o}{A}B_1 \sin(\omega_m t) + \left[\frac{(k_2-k_1)B_1^2}{4A}\cos 2\omega_m t\right] + \left[\text{D.C. TERMS}\right]$$

WITH $\frac{B_o}{B_1} \leq 0.1$, $\frac{B_1}{A} \leq 0.1$, $\frac{k_1-k_2}{k_1+k_2} < 0.05$;

$$\Longrightarrow \frac{(k_1-k_2)}{(k_1+k_2)}\frac{B_o}{A} < 5 \times 10^{-4}$$

Fig. 6. Summary of the phase detection method.

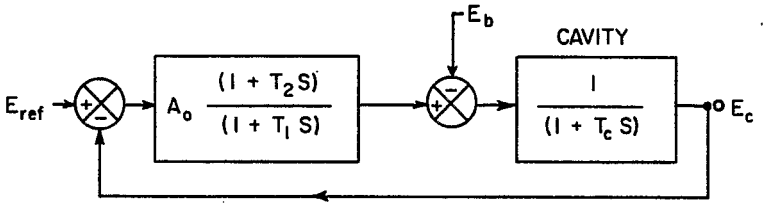

FOR $T_2 \approx T_c$

$$E_c \cong \frac{E_{ref}}{\frac{(1 + T_1 S)}{A_o}} - \frac{E_b (1 + T_1 S)}{A_o \frac{(1 + T_1 S)}{A_o} (1 + T_c S)}$$

$$T_c = \frac{2 Q_L}{\omega_o} \simeq 0.032 \text{ sec}$$

$$A_o \simeq 10^5$$

GAIN-BANDWIDTH $\simeq$ 10kHz $\Rightarrow$ $T_1 \approx 1.6$ sec

Fig. 7. Loop transfer functions for the amplitude control loop. The cavity voltage E_c is given in terms of the reference voltage E_{ref} and the beam-induced voltage E_b.

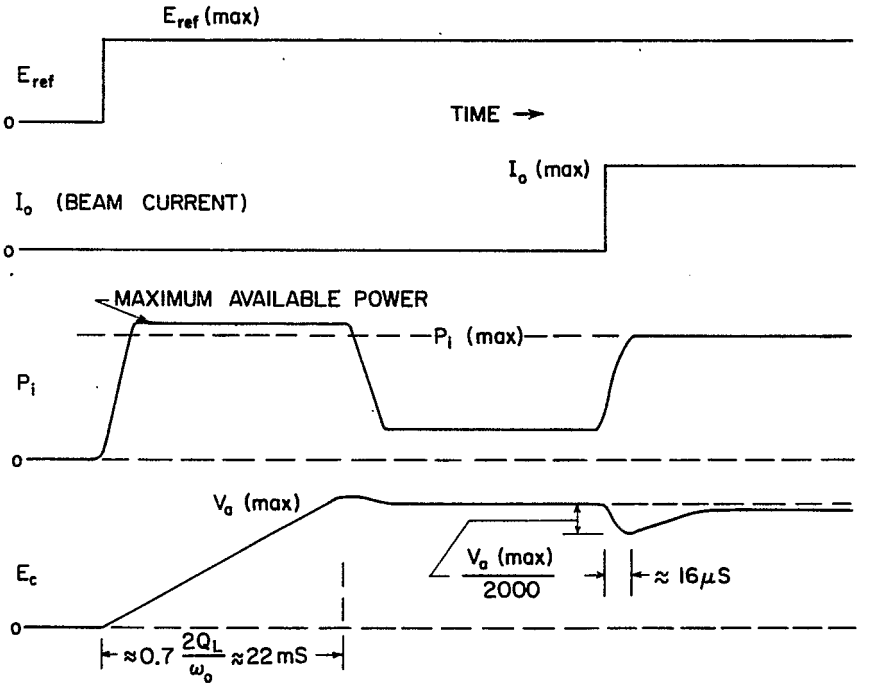

Fig. 8. Expected time response of the cavity voltage E_c and the incident power P_i during the turn-on of the reference voltage and beam current. Conditions are shown for the beam current I_o(max) and the cavity voltage V_a(max).

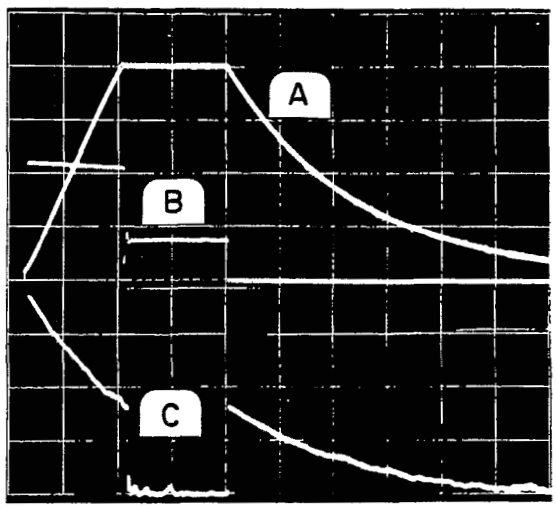

Fig. 9. Oscilloscope traces obtained during a recent test with a pulsed reference voltage on a superconducting cavity structure. Trace (A) is the cavity voltage, trace (B) is the square root of the incident power (linear detectors), and trace (C) is the square root of the reflected power from the cavity structure. The time scale is 5 msec per division.